Bull. Chem. Soc. Jpn., 77, 2121–2127 (2004)

Dopants for a Perfluorinated Graded Index Polymer Optical Fiber

Masaki Naritomi,* Hidenobu Murofushi, and Naotoshi Nakashima[1,†]

Lucina division, Asahi Glass Co., Ltd., 1-12-1, Yurakucho, Chiyoda-ku, Tokyo 100-8205

[1]Department of Materials Science, Graduate School of Science and Technology, Nagasaki University,
Bunkyo, Nagasaki 852-8521

Received May 18, 2004; E-mail: masaki-naritomi@agc.co.jp

A perfluorinated graded index polymer optical fiber (PFGI-POF) has been developed and manufactured for data communication to provide a high bandwidth with easy termination and cabling. In the PFGI-POF technology, the graded refractive index profile using dopants is a key technology to obtain a high bandwidth, excellent transparency and thermal durability. This study of the dopant selection for the PFGI-POF is reported for the first time.

The technology of graded index polymer optical fibers, developed in the 1990s and 2000s has enabled the manufacture of high bandwidth fibers that offer reduced wiring cost due to the ease of termination and cabling for short haul data communication.[1–3] In particular, perfluorinated graded index polymer optical fibers (PFGI-POF) were developed and manufactured for short-medium haul data communication in order to obtain especially low optical attenuation and high bandwidth in the near IR region and high bandwidth due to the superior optical properties of the perfluorinated polymer compared to the polymethylmethacrylate (PMMA)-based polymer optical fiber.[4,5] The factors affecting the attenuation loss of the polymer optical fibers are summarized in Scheme 1.[6]

With regard to these factors, the absorption in the near IR region is primarily related to the vibrational overtones of the stretching bonds in the molecule. The absorption losses due to the overtone vibration of the carbon–hydrogen (C–H), carbon-deuterium (C–D), and carbon–fluorine (C–F) bonds in the polymer have been approximated by Groh.[7] In order to realize low attenuation in the near IR region, the perfluorinated polymer (PF polymer) as shown in Fig. 1 is an ideal polymer. It is amorphous with a glass transition temperature (T_g) of 108 °C and has no C–H bonds, no carbon–oxygen double (C=O) bonds and no oxygen–hydrogen (O–H) bonds.[8]

- Intrinsic
  - Absorption
    - Vibrational overtone
    - Electron transition
  - Scattering
    - Crystal
    - Rayleigh scattering
- Extrinsic
  - Absorption
    - Transition metal
    - Impurities (organic)
  - Scattering
    - Impurities (gas)
    - Structural imperfection

Scheme 1. The optical attenuation factors in polymer optical fiber.

The refractive index raising dopant is the key material needed to obtain a graded index profile in PFGI-POF. The critical performance properties of the fiber, including high bandwidth, low attenuation, and thermal durability, all depend on the choice of dopant. However in the case of PFGI-POF, dopant selection is more difficult than for PMMA or other polymer fibers due to the low solubility of suitable dopants in the PF polymer.

For an excellent dopant selection, the performance criteria of the dopant are as follows: 1) Its molecular size should be smaller than 1/10 the utilized wavelength; 2) It should have no serious absorption in the visible and near IR regions; 3) It should have no serious scattering loss caused by the structural imperfection in the PF polymer, as shown in Fig. 1; 4) It must be miscible in the PF polymer; 5) It must have a higher refractive index than the PF polymer ($n = 1.342$ for the polymer of Fig. 1); The refractive index of the core (n_1) should be at least 0.015 higher than that of the desired cladding (n_2), as shown in Fig. 2; and 6) the T_g at the core center of PFGI-POF should be higher than 90 °C in order to obtain the thermal durability

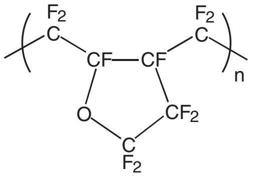

Fig. 1. Chemical structure of the perfluorinated polymer.

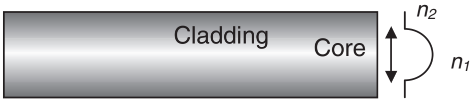

Fig. 2. Conceptual diagram of the PFGI-POF.

[†] Present address: Department of Chemistry and Biochemistry Graduate School of Engineering, Kyushu University, Hakozaki 6-10-1, Fukuoka 821-8581

Published on the web November 11, 2004; DOI 10.1246/bcsj.77.2121

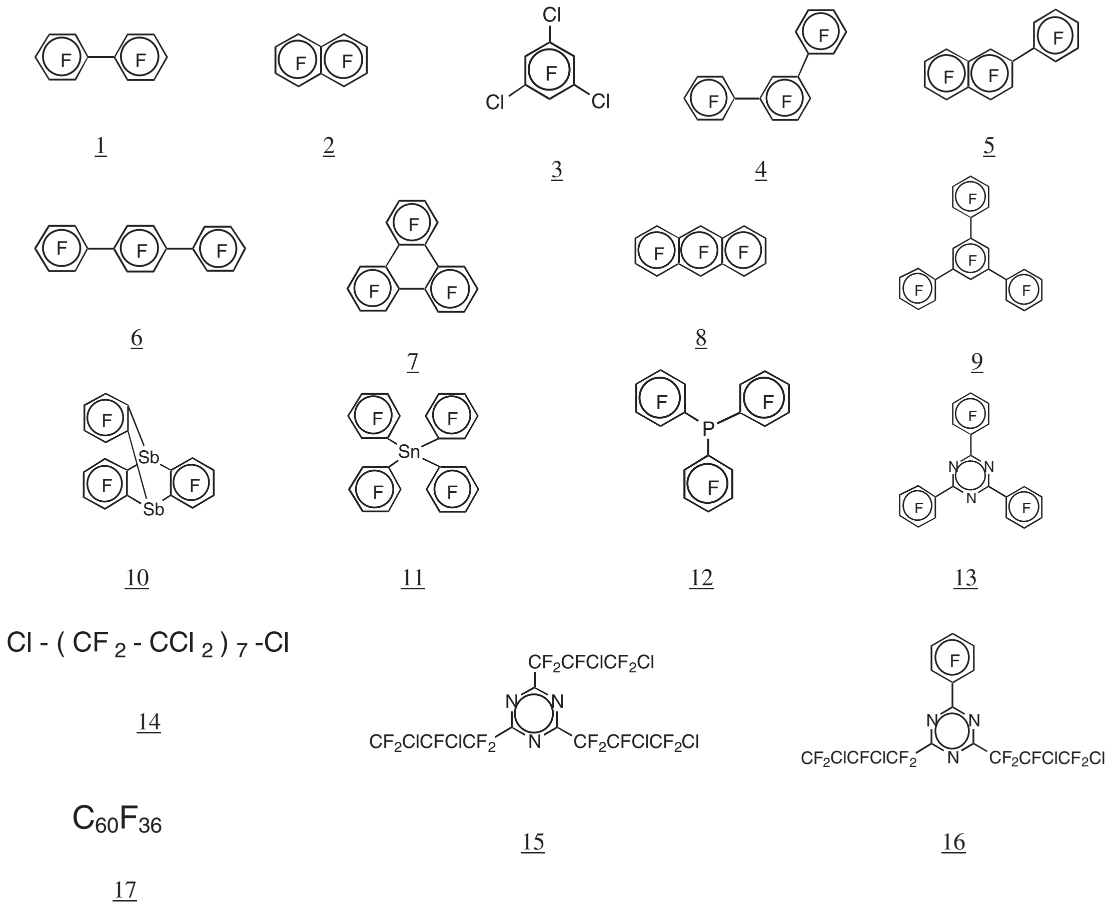

Fig. 3. Chemical structure of the dopants in this study.

when the numerical aperture (NA) calculated in Eq. 1 of the PFGI-POF is 0.20.

$$\mathrm{NA} = \sqrt{n_1^2 - n_2^2}. \tag{1}$$

Because the dopants are usually crystalline, the T_g of the dopant is not directly measured; therefore, the T_g is estimated by the Fox equation (Eq. 2),[9]

$$1/T_{g_{\mathrm{blend}}} = w_D/T_{g_D} + w_P/T_{g_P} \tag{2}$$

where $T_{g_{\mathrm{blend}}}$ is the glass transition temperature of the doped polymer, w_D and w_P are weight percents of dopant and polymer, and T_{g_D} and T_{g_P} are the glass transition temperatures of dopant and polymer. From this Fox equation (Eq. 2), one sees that decreasing the concentration of dopant and/or increasing the T_g of the dopant produces a higher T_g at the core center of the PFGI-POF. The higher solubility of the dopant in the PF polymer, and a high T_g and high refractive index of the dopant are the first control gate for the dopant selection. For a high solubility, the dopant must be a fluorinated molecule. For a higher T_g and refractive index, the dopant should have a higher molecular weight, for example due to heavy atoms, such as chlorine (Cl), or bromine (Br), or alternatively, one or more aromatic rings. In this study, the fluorinated molecules including those with aromatic rings and Cl were synthesized and evaluated.

Experimental

Materials. The following materials shown in Fig. 3 were purchased and purified. A chlorotrifluoroethylene oligomer was purchased from Mihama Co. and distilled before evaluation. The main fraction was composed of $Cl(CF_2CFCl)_7Cl$ (**14**). Perfluorobiphenyl (**1**), perfluoronaphthalene (**2**), 1,3,5-trichloro-2,4,6-trifluorobenzene (**3**), and perfluorotriphenylphosphine (**12**) were purchased from Kanto Chemical Co. and $C_{60}F_{36}$ (**17**) was purchased from Tokyo Progress System Co. In order to make PFGI-POF, further purifications such as recrystallization or sublimation were conducted to increase the purities (>99%). Purity was analyzed by gas chromatography using a DB1301 column in acetone solution.

Other materials shown in Fig. 3 were already known and were prepared according to the literature, as described below:

Perfluoro-*m*-terphenyl (4):[10] 1,3-Dibromotetrafluorobenzene (10 g), bromopentafluorobenzene (50 g), activated copper bronze (50 g), and dimethylformamide (100 mL) were refluxed together for 5 h. The mixture was filtered and the solid was washed twice with hot dimethylformamide (500 mL). The combined filtrate was added to water (1000 mL) and the precipitated solid (25 g) was collected, dried, and heated in vacuum to sublime the perfluoro-*m*-terphenyl. It was recrystallized twice from hexane to give perfluoro-*m*-terphenyl in 12% yield. The material was identified by GC mass spectrometry (a parent ion peak at $m/z = 482$ with a cracking pattern consistent with the objective structure). GC purity 99.5%. Mp. 127 °C.

Perfluoro-(2-phenylnaphthalene) (5): Mg (8 g), I_2 (0.05 g), and tetrahydrofuran (1 L) were placed in a 2 L flask. Bromopentafluorobenzene (82 g) was added in the flask at 5–20 °C for 1 h (Solution A). Perfluoronaphthalene (45 g) and tetrahydrofuran (500 mL) were placed in another flask. Solution A was added in the mixture and heated at 65 °C for 8 h. 2M HCl water (600 mL) was added and the precipitated solid was washed with water, and dried. The solid was subjected to fractional vacuum sublimation. At 150 °C perfluoro-(2-phenylnaphthalene) was obtained. The yields were 15%. The material was identified by GC mass spectrometry (parent ion peaks at $m/z = 420$ with a cracking pattern consistent with the objective structure). GC purity 99.2%. Mp. 89 °C.

Perfluoro-*p*-terphenyl (6):[11] Mg (36.5 g) and tetrahydrofuran (800 mL) were placed in a 2 L flask. Bromopentafluorobenzene (370 g) was slowly added in the flask, and the solution was stirred at 30 °C for 6 h (Solution B). Perfluorobiphenyl (334 g) and tetrahydrofuran (2 L) were put in another 5 L flask. Solution B was added in the flask at 15 °C for 1 h and stirred at 30 °C for 20 h. The mixture was poured into water, and the precipitated solid was washed with water and dried. The obtained solid was subjected to fractional vacuum sublimation. At 140 °C, perfluoroterphenyl was obtained as white crystals in 10% yield. The material was identified by GC mass spectrometry (a parent ion peak at $m/z = 482$ with a cracking pattern consistent with the objective structure). GC purity 99.8%. Mp. 194 °C.

Perfluorotriphenylene (7):[12] 1,2-Diiodotetrafluorobenzene (10 g) and copper powder (10 g) were heated at 200 °C for 50 h in a sealed evacuated tube. The contents were then extracted with ether, the solution was filtered and the ether was removed at 0 °C to give a solid that was subjected to fractional vacuum sublimation. Dodecafluorotriphenylene sublimed at 140 °C and was recrystallized from hexane. The yields were 18%. The material was identified by GC mass spectrometry (parent ion peaks at $m/z = 444$ with a cracking pattern consistent with the objective structure). GC purity 99.1%. Mp. 108 °C.

Perfluoroanthracene (8):[13] 9,10-Dichloroanthracene (20 g), KF (9.8 g), sulfolane (100 mL), and toluene (200 mL) were placed in a 1 L flask. The mixture was heated at 118 °C for 2 h. Toluene was removed from the top of the flask and the flask was heated at 210 °C for 4 h. Water was added in the flask, the obtained solid was filtered, and then washed twice with water, and dried. The solid was recrystallized from chloroform. The perfluoroanthracene was obtained as a pale yellow powder in 56% yield. Mp. 208 °C. The material was identified by GC mass spectrometry (a parent ion peak at $m/z = 358$ with a cracking pattern consistent with the objective structure). GC purity 99.0%.

Perfluoro-1,3,5-triphenylbenzene (9):[14] Bromopentafluorobenzene (148 g) and tetrahydrofuran (500 mL) were placed in a 2 L flask. 1 mol/L ethylmagnesium bromide in tetrahydrofuran solution (600 mL) was added to the flask at 5 °C for 2 h. CuI (172 g) was added in the mixture while maintaining the temperature below 10 °C. 1,4-Dioxane (200 mL) was added to the flask and the mixture was stirred for 30 min. 1,3,5-Trifluorotriiodobenzene was quickly added to the flask. The flask was heated at 70 °C for 20 h. The mixture was poured into water and the precipitated solid was extracted by hot hexane and recrystallized twice from hexane. Perfluoro-1,3,5-triphenylbenzene was obtained as a white crystal in 43% yield. The material was identified by GC mass spectrometry (a parent ion peak at $m/z = 630$ with a cracking pattern consistent with the objective structure). GC purity 99.9%. Mp. 152 °C.

$Sb_2(C_6F_4)_3$ (10):[15] Powdered antimony (3 g) and 1,2-diiodotetrafluorobenzene (3 g) were heated together in a sealed tube at 250 °C for 24 h. The tube was cut open and the solid product was crushed to a powder before being extracted with ether. The solution was filtered and the ether was removed to give a solid. After the fractional vacuum sublimation, $Sb_2(C_6F_4)_3$ was obtained. It was recrystallized from hexane. The yield was 21%. It was identified by GC mass spectrometry (a parent ion peak at $m/z = 686$ with a cracking pattern consistent with the objective structure). GC purity 98.5%. Mp. 268 °C.

Perfluoro(tetraphenyl) Tin (11):[16] Mg (2.5 g), I_2 (0.01 g), and tetrahydrofuran (200 mL) were placed in a 500 mL flask. Bromopentafluorobenzene (25 g) was added in the flask at 5–20 °C for 1 h. Anhydrous tin tetrachloride (26 g) was added to the mixture and the combination was heated at 65 °C for 10 h. 2M HCl aqueous solution (100 mL) was added and the precipitated solid was washed with water, and dried. The solid was recrystallized from chloroform; perfluoro(tetraphenyl) tin was obtained in 56% yield. The material was identified by GC mass spectrometry (a parent ion peak at $m/z = 787$ with a cracking pattern consistent with the objective structure). GC purity 99.2%. Mp. 221 °C.

2,4,6-Tris(pentafluorophenyl)-1,3,5-triazine (13):[17] Pentafluorobenzonitrile (150 g) and fluorosulfuric acid (500 g) were placed in a 1 L glass flask with stirring at room temperature for 7 days. The mixture was poured into cold water with ice (3 L) and the precipitated solid (132 g) collected, washed with water, and dried. The solid was recrystallized twice from toluene. 2,4,6-Tris(pentafluorophenyl)-1,3,5-triazine was obtained as a white crystal in 46% yield. The material was identified by GC mass spectrometry (a parent ion peak at $m/z = 579$ with a cracking pattern consistent with the objective structure). GC purity 99.8%. Mp. 123 °C.

2,4,6-Tris(2′,3′-dichloro-1′,1′,2′,3′,3′-pentafluoropropyl)-1,3,5-triazine (15):[18] 3,4-Dichloro-2,2,3,4,4-pentafluorobutanenitrile (288 g) and 2-ethylhexylamine (8.2 g) were placed in a 500 mL flask. The mixture was heated at 90–150 °C for 7 days. The product was distilled at 3 mmHg at 100–102 °C, washed twice with water, and dried. After distillation again in 3 mmHg vacuum, 2,4,6-tris(2′,3′-dichloro-1′,1′,2′,3′,3′-pentafluoropropyl)-1,3,5-triazine was obtained as a colorless liquid in 48% yield. The material was identified by GC mass spectrometry (a parent ion peak at $m/z = 681$ with a cracking pattern consistent with the objective structure). GC purity 99.3%.

2,4-Bis(2′,3′-dichloro-1′,1′,2′,3′,3′-pentafluoropropyl)-6-pentafluorophenyl-1,3,5-triazine (16):[18] 3,4-Dichloro-2,2,3,4,4-pentafluorobutanenitrile (45 g) and NH_3 were placed in a 100 mL stainless steel autoclave. The contents of the reactor were stirred at 30 °C for 5 days. After the NH_3 was purged, the product was placed in another 200 mL flask. 3,4-Dichloro-2,2,3,4,4-pentafluorobutanenitrile (40 g) was slowly added in the flask at 50 °C for 1 h, and pentafluorobenzoyl chloride (46 g) was slowly added. After heating at 50 °C for 4 h, the product was poured into water and dried. The liquid was distilled at 3 mmHg and 128–130 °C, 2,4-bis(2′,3′-dichloro-1′,1′,2′,3′,3′-pentafluoropropyl)-6-pentafluorophenyl-1,3,5-triazine was obtained in 62% yield. The material was identified by GC mass spectrometry (a parent ion peak at $m/z = 647$ with a cracking pattern consistent with the objective structure). GC purity 99.2%.

The test methods described below were used in this study.

Blending Test, Mixing the Perfluorinated Polymer and the Dopants. The miscibility of the dopants in the perfluorinated polymer and T_g at the composition corresponding to the fiber core

Table 1. The Characteristics of the Dopants and the Results of the Blend Testing

Dopant	Molecular weight	T_g/°C	Refractive index (n_D)	Solubility /wt %	PFGI-POF (NA = 0.20)	
					T_g at core/°C	Dopant conc./wt %
1	334	−115	1.465	15	70.6	13.5
2	272	−110	1.478	10	73.4	7.4
3	236	−110	1.492	6	76.6	6.4
4	482	−80	1.471	20	82.3	7.4
5	420	−125	1.514	15	79.0	5.5
6	482	−65	1.487	7	88.9	6.4
7	444	−82	1.531	10	91.5	4.9
8	358	−60	1.562	4	94.8	4.4
9	630	−70	1.471	10	84.1	7.4
10	687	−75	1.533	4	92.3	4.9
11	787	−50	1.482	7	91.7	6.4
12	688	−75	1.504	14	90.2	5.9
13	579	−55	1.528	7	94.0	5.3
14	1002	−45	1.413	17	77.4	13.5
15	681	−70	1.413	20	68.6	13.5
16	647	−85	1.445	15	75.5	9.3
17	1404	0	1.589	1	99.2	3.5

center for NA = 0.20 were evaluated using a blend test as shown in Table 1. The blend test was carried out using spontaneous mixing of the molten perfluorinated polymer and the liquid dopant in a sealed glass tube by heating at 270 °C for 3 days. After cooling to room temperature, the T_g of the blended polymer, for which $n = 1.355$ (NA = 0.20), was observed by TMA analysis using a pressed film. For each 1 wt % dopant concentration increment, the mixture was checked for phase separation, indicated by the onset of opacity, observed using visual inspection. The solubility limit of the dopants in the perfluorinated polymer was determined using this observation, as shown in Table 1. In addition, the T_g of the dopant was calculated using the Fox equation (Eq. 2), as shown in Table 1.

Refractive Index Measurements. The refractive indices of both the pure and the doped polymers were measured on pressed films (10 mm × 40 mm × 0.2 mm) using an Abbe refractometer.

T_g Measurements. The glass transition temperatures were measured by TMA analysis using pressed films (2 mm × 20 mm × 0.2 mm).

Light Scattering Measurements. Scattering intensities, Vv and Hv, were measured using a light scattering photometer SLS-6000HL produced by Otsuka Electronics. The rod sample that was used for the measurement had a 22 mm outer diameter and a 70 mm length. The measurement was transformed into scattering loss (dB/km) using the following equation:

$$\alpha_{\text{scattering}}\ (\text{dB/km}) = 10\log e\pi \int [(1+\cos 2\theta)\text{Vv} + (2+\sin 2\theta)\text{Hv}]\sin\theta\, d\theta\ (\text{cm}^{-1}) \times 10^5. \qquad (3)$$

Attenuation Measurements. The optical attenuation of PFGI-POF was measured by the conventional cutback method, using a monochrometer to scan wavelength.

Index Profile Measurements. The refractive index profiles of PFGI-POF were measured using the interference microscopic method.

Results and Discussion

The chemical structures of all dopants in this study are shown in Fig. 3. The molecular weight, calculated T_g value of the dopant, refractive index, and wt % solubility in the PF polymer of each dopant are shown in Table 1. The T_g at core center of a PFGI-POF for the case where NA = 0.20 and the wt % concentration of the dopant for this case are also shown in Table 1.

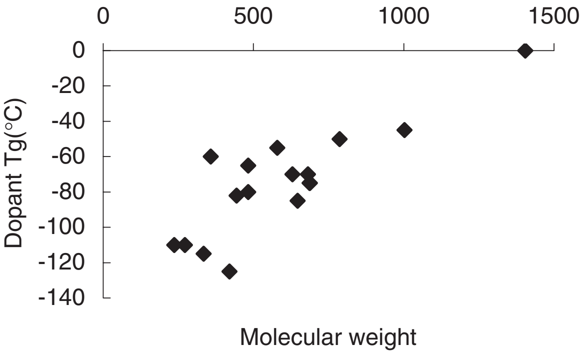

Fig. 4. Plots of the relationships between molecular weight and dopant's T_g.

For the study of dopant selection, the molecular weight dependence of each dopant's T_g is plotted in Fig. 4. The lightweight molecules have a low T_g in general. However, an exception to this trend is a lightweight molecule which has a fluorobenzyl, which seems to have a higher T_g.

The refractive index dependence of the dopant solubility in the PF polymer is plotted in Fig. 5. **14**, **15**, and **16**, which include chlorotrifluoroethylene groups, attain 15–20 wt % solubility, a good result. In the cases of **15** and **16**, the triazine and benzyl ring effect no obvious refractive index improvement. **4**, **5**, **7**, **8**, and **12** have higher solubilities if one compares dopants with the same refractive index.

In order to evaluate the structural effect on the refractive index and the solubility in more detail, we compare the dopants **1**, **4**, and **9**, which are composed of two, three, and four fluorobenzyl rings. These dopants show similar refractive indices

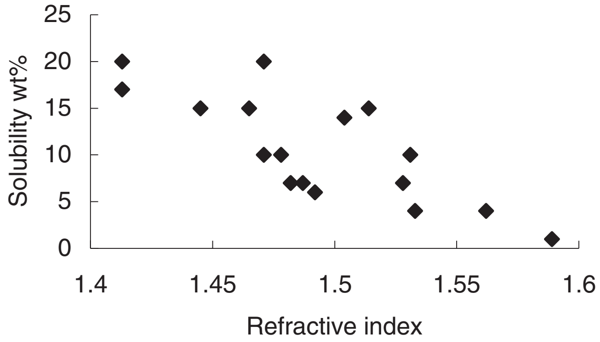

Fig. 5. Plots of the relationships between refractive index and solubility of dopants.

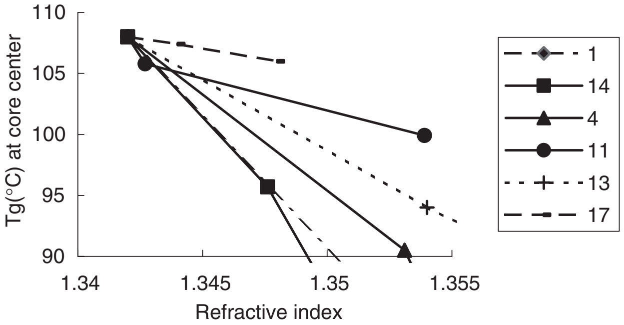

Fig. 6. Dopant concentration dependence of refractive index and T_g at core center of PFGI-POF.

but different solubilities. The reason why **4** shows a higher solubility compared to those of **1** and **9** is not evident. Comparing **2** and **8**, one sees that the refractive index of the dopant depends strongly on the number of conjugated double bonds. The chemically similar **4**, **5**, **6**, **7**, and **8**, which have three fluorobenzyl rings and similar molecular weights, are compared further. **8** and **7**, which are composed of continuous conjugated double bonds, attain a higher refractive index. On the other hand, increasing the number of fluorine atoms effects a higher solubility. Among **4**, **5**, **7**, and **8**, with the exception of perfluoro-*p*-terphenyl (**6**), the dopant solubility is proportion to the number of fluorine atoms in the molecule. Comparing **5** and **7** which having same numbers of fluorine atoms, one sees that **7** has low solubility due to its large cubic volume. **6** also has a low solubility due to its large cubic volume. If one considers the two cases, cubic volume seems to effect the dopant solubility more than the number of fluorine atoms. From the standpoint of dopant selection for high T_g, high solubility, and high refractive index, perfluoro-*m*-terphenyl (**4**) is well balanced with respect to both high solubility and high refractive index, due to its minimized cubic volume and evenly turned-out fluorine atoms. However **4** does not achieve the required performance 6) of T_g at the fiber core center for temperatures greater than 90 °C.

To achieve the higher T_g, high solubility and high refractive index, we evaluated the dopants **10**, **11**, **12**, and **13**, which are composed of phosphate, tin, antimony, and triazine as a center atom connecting three or four fluorobenzyl. However, **10** could not be dissolved at 4.9 wt % in the PF polymer to give the the NA = 0.2 condition and **12** became colored at the fiber fabrication temperature over 300 °C.

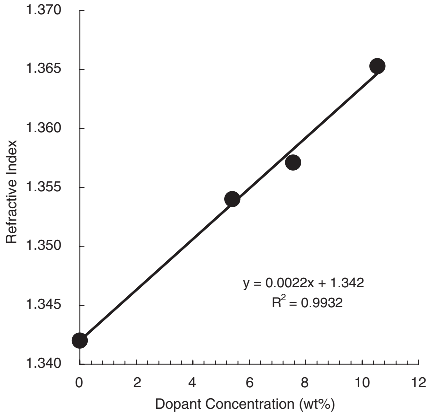

Fig. 7. Plots of dopant concentration dependence of the doped polymer's refractive index using **13**.

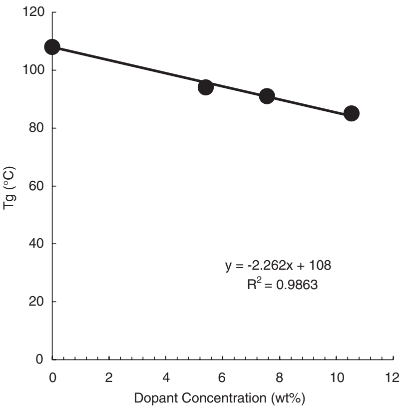

Fig. 8. Plots of dopant concentration dependence of the doped polymer's T_g using **13**.

Of the required performances discussed in the introduction, the conditions 5) and 6) are the most important after the first gate for the dopant selection. Dopant concentration affects the degradation of T_g and the refractive index at the center core of PFGI-POF. The results of the dopant concentration dependence on T_g in the cases of **1**, **4**, **11**, **13**, **14**, and **17** are shown in Fig. 6.

11 and **13** are acceptable based on conditions 5) and 6). **17** is not dissolved at the condition of the refractive index = 1.355. **11** is a strong poison, and consequently it is not acceptable. Therefore 2,4,6-tris(pentafluorophenyl)-1,3,5-triazine (**13**) is selected as the candidate for the dopant in PFGI-POF in this study. The relationships between the concentration of **13** and the refractive index or T_g of the polymer-dissolved dopant (doped polymer) are shown in Figs. 7 and 8. The temperature dependences of the refractive index for both the PF polymer and the doped polymer are evaluated as shown in Fig. 9.

The estimated scattering loss results of the PF polymer and the doped PF polymer at 633 nm and 850 nm wavelength are shown in Table 2. These results are calculated using the Hv and Vv intensity data of the light scattering measurement as shown in Fig. 10. The results in Fig. 10 suggest that the PF polymer has an entirely homogeneous and amorphous morphology, as in the case of PMMA. However the doped PF

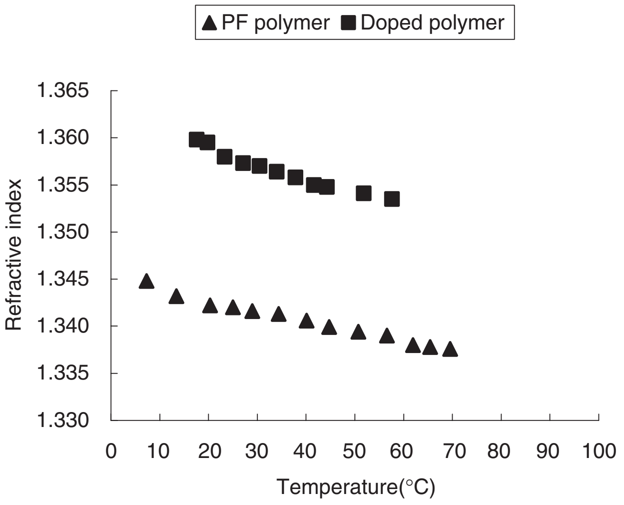

Fig. 9. Plots of temperature dependence of the refractive index of the PF polymer and the doped polymer using **13**.

Table 2. Estimated Scattering Loss (dB/km) of the PF Polymer and the Doped Polymer at 633 nm and 850 nm Wavelength

Wavelength	633 nm			850 nm
Scattering loss	$\alpha^{\rm iso}$	$\alpha^{\rm aniso}$	$\alpha^{\rm total}$	$\alpha^{\rm total}$
PF polymer	5.4	4.1	9.5	2.9
Doped PF polymer	24.0	9.7	33.7	11.5

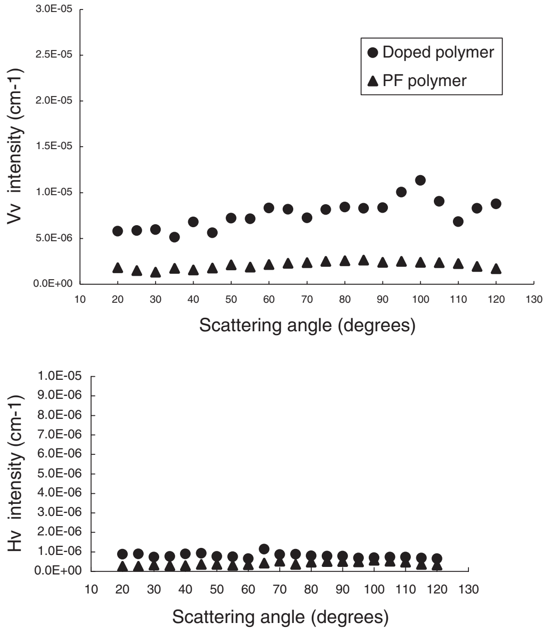

Fig. 10. Hv and Vv intensity data of the PF polymer and the doped polymer by the light scattering measurement.

polymer exhibits excess scattering loss compared to the PF polymer. The excess scattering loss is caused by the structural imperfection of the doped PF polymer, due to the low dopant solubility of about 10% that leads to imperfectly dissolved dopant in the PF polymer.

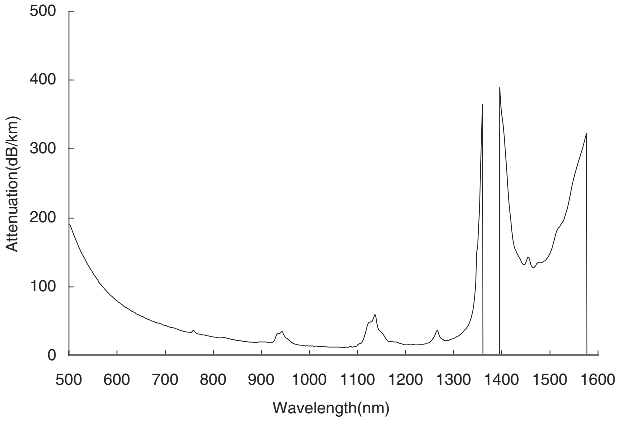

Fig. 11. The attenuation loss measurement results of PFGI-POF in near infrared region.

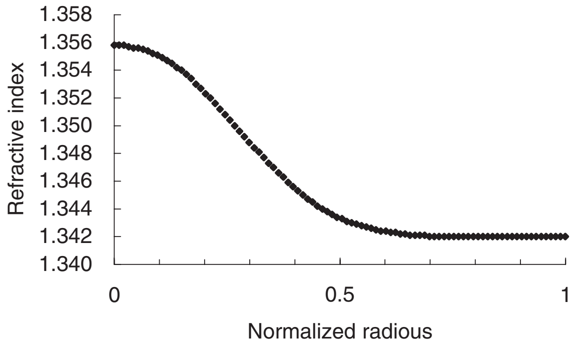

Fig. 12. The index profile measurement results from core center to outer diameter of PFGI-POF.

For the evaluation of the optical attenuation and the capability of forming a suitable index profile, the PFGI-POF using the dopant **13** was fabricated and evaluated. The attenuation in the near infrared region and the index profile from center to outer diameter of the PFGI-POF are shown in Figs. 11 and 12.

The shape of the index profile in Fig. 12 is typical of that formed by thermal diffusion of a dopant in the polymer. The attenuation of PFGI-POF is 15–20 dB/km at 850 nm, which is not only close to the estimated attenuation in Table 2 but also the lowest attenuation recorded in a polymer optical fiber. Despite this excellent result, the solubility and miscibility of **13** in the PF polymer should be improved to reduce the excess scattering loss in order to obtain a reduced attenuation for PFGI-POF.

Conclusion

In total, seventeen dopants for PFGI-POF were evaluated in this study. In accord with the required performance of the dopant described in the introduction, the best candidates among these dopants were perfluoro(tetraphenyl) tin (**11**) and 2,4,6-tris(pentafluorophenyl)-1,3,5-triazine (**13**). Both candidates have several fluorobenzyl groups, which are the most effective moiety for increasing the refractive index and T_g of the doped polymer compared to chlorinated (Cl) compounds. Because of the hazardous nature of **11**, **13** was selected as the most effective dopant for PFGI-POF in this study. However the solubility and miscibility of the dopant in the PF polymer should be further improved to reduce the excess scattering, and improve the attenuation characteristics of PFGI-POF.

This work was a collaboration involving Nagasaki University and Keio University. We appreciate all members of both groups, especially Prof. Koike of Keio University. We also appreciate all members who are in charge of the Lucina project, especially Mr. C. Tanaka, Mr. T. Matsuyama, Mr. Y. Watanabe, Mr. Y. Takano, Mr. T. Tsukamoto, Mr. T. Onishi, Mr. K. Koganezawa, Mr. K. Chiba, Mr. K. Kurashima, Mr. G. Ogawa, Mr. T. Okazoe, Mr. M. Ito, Mr. Y. Takebe, Mr. J. Irisawa, Mr. S. Tatematsu, Mr. M. Tamura, Mr. N. Sakata, and Mr. N. Sugiyama at Asahi Glass Co. Ltd.

References

1 Y. Koike, T. Ishigure, and E. Nihei, *J. Lightwave Technol.*, **13**, 1475 (1995).

2 T. Ishigure, E. Nihei, and Y. Koike, *Appl. Opt.*, **35**, 2048 (1996).

3 T. Ishigure, M. Satou, O. Takanashi, E. Nihei, T. Nyu, S. Yamasaki, and Y. Koike, *J. Lighwave Technol.*, **15**, 2095 (1997).

4 T. Ishigure, S. Tanaka, E. Kobayashi, and Y. Koike, *J. Lighwave Technol.*, **20**, 1449 (2002).

5 T. Ishigure, Y. Koike, and J. W. Fleming, *J. Lighwave Technol.*, **18**, 178 (2000).

6 T. Kaino, K. Jinguji, and S. Nara, *Appl. Phys. Lett.*, **42**, 567 (1983).

7 W. Groh, *Makromol. Chem.*, **189**, 2861 (1988).

8 M. Nakamura, T. Kawasaki, M. Unoki, K. Oharu, N. Sugiyama, I. Kaneko, and G. Kojima, *Prog. Pac. Polym. Sci., Proc. Pac. Polym. Conf., 1st*, **1991**, Meeting Date 1989, 369.

9 T. G. Fox, *Bull. Am. Phys. Soc.*, **1**, 123 (1956).

10 J. Thrower and M. A. White, *Polym. Prepr.*, **7**, 1077 (1966).

11 K. Maruo, Y. Wada, and S. Yanagida, *Bull. Chem. Soc. Jpn.*, **65**, 3439 (1992).

12 R. D. Chambers, C. J. Skinner, M. Atherton, and J. S. Molliet, *J. Chem. Soc., Chem. Commun.*, **1995**, 19.

13 a) J. Burdon, A. C. Childs, I. W. Persons, and J. C. Tatlow, *J. Chem. Soc., Chem. Commun.*, **1982**, 534. b) G. G. Yakobson, V. N. Odinokov, and N. N. Vorozhtsov, *Tetrahedron Lett.*. **6**, 4473 (1965). c) Japan Patent H11-12203. d) Japan Patent H11-12204.

14 a) J. Porwisiak and M. Schlosser, *Chem. Ber.*, **129**, 233 (1996). b) Japan Patent S64-25737.

15 a) N. A. A. Al-Jabar and A. G. Massey, *J. Organomet. Chem.*, **276**, 331 (1984). b) T. K. Mistry and A. G. Massey, *J. Organomet. Chem.*, **209**, 45 (1981). c) W. R. Cullen and A. W. Wu, *J. Fluorine Chem.*, **8**, 183 (1976).

16 J. M. Holmes, R. D. Peacock, and J. C. Tatlow, *J. Chem. Soc.*, **1966**, 150.

17 A. O. Miller and G. G. Furin, *Mendeleev Commun.*, **5**, 166 (1994).

18 a) H. C. Brown and M. T. Cheng, *J. Chem. Eng. Data*, **13**, 560 (1968). b) US Patent 3654273. c) Japan Patent H09-3027.